Journal of Molecular Neuroscience (2021) 71:746–760
https://doi.org/10.1007/s12031-020-01694-6

Regeneration of Rat Sciatic Nerve Using PLGA Conduit Containing Rat ADSCs with Controlled Release of BDNF and Gold Nanoparticles

Maliheh Jahromi[1] · Shahnaz Razavi[1] · Reihaneh Seyedebrahimi[1] · Parham Reisi[2] · Mohammad Kazemi[3]

Received: 4 July 2020 / Accepted: 28 August 2020 / Published online: 7 October 2020

Abstract

Implantation of a nerve guidance conduit (NGC) carrying neuroprotective factors is promising for repairing peripheral nerve injury. Here, we developed a novel strategy for repairing peripheral nerve injury by gold nanoparticles (AuNPs) and brain-derived neurotrophic factor (BDNF)–encapsulated chitosan in laminin-coated nanofiber of Poly(l-lactide-co-glycolide) (PLGA) conduit and transplantation of rat adipose–derived stem cells (r-ADSCs) suspended in alginate. Then, the beneficial effect of AuNPs, BDNF, and r-ADSCs on nerve regeneration was evaluated in rat sciatic nerve transection model. In vivo experiments showed that the combination of AuNPs- and BDNF-encapsulated chitosan nanoparticles in laminin-coated nanofiber of PLGA conduit with r-ADSCs could synergistically facilitate nerve regeneration. Furthermore, the in vivo histology, immunohistochemistry, and behavioral results demonstrated that the AuNPs- and BDNF-encapsulated chitosan nanoparticles in NGC could significantly reinforce the repair performance of r-ADSCs, which may also contribute to the therapeutic outcome of the AuNPs, BDNF, and r-ADSCs strategies. In this study, we found that the combination of AuNPs and BDNF releases in NGC with r-ADSCs may represent a new potential strategy for peripheral nerve regeneration.

Keywords Adipose-derived stem cells · Brain-derived neurotrophic factor · Controlled release · Gold nanoparticle · Poly(L-lactide-co-glycolide) · Nerve conduit

Introduction

Peripheral nerve injuries can be caused by accidental lacerations, congenital defects, surgical intervention, and neuropathies such as infections, inherited problems, metabolic causes, and exposure to toxins. In addition, nerve damages can lead to symptoms of neuropathic pain, atrophy of the target skeletal muscles, and partial or even complete loss of motor and sensory functions (Baltzis et al. 2018; Faroni et al. 2015). In the most severe form of injury is a full transection of the axons and myelin sheaths wherein complete discontinuity or gap of the nerve is observed (Campbell 2008). These types of injuries are very hard to treat and are still a challenging clinical problem.

Autologous nerve graft represents the clinical gold standard to fill the large nerve gaps and make the junction between the distal and proximal stumps of the injured nerves.

However, an autograft is limited due to a second surgery to isolate the donor nerve graft, scar formation at the donor site, limited nerve graft availability, mismatch of donor nervous tissue geometrics and size, and the possibility of neuroma formation (Gaudin et al. 2016).

In dealing with such limitations, an alternative approach for nerve autograft replacement is artificial nerve guidance conduits (NGCs). Moreover, NGC reduces neuronal apoptosis, neuroma formation, axonal escape, donor site morbidity, and muscle atrophy during peripheral nerve regeneration but is limited by range (≤ 3 cm) and low functional recovery rates (Pabari et al. 2014). In addition, the difference between autologous nerve grafts and NGCs is that Schwann cells within autografts can express several types of neurokines and cell adhesion molecules to promote axon regeneration and myelin formation. It indicates that the combination of NGCs, neurokines, and stem cells could mimic the environment of autologous nerve grafts and might be efficient in repair of peripheral nerve injury (Patel et al. 2018).

✉ Shahnaz Razavi
razavi@med.mui.ac.ir

[1] Department of Anatomical Sciences, School of Medicine, Isfahan University of Medical Sciences, Isfahan 81744176, Iran

[2] Department of Physiology, School of Medicine, Isfahan University of Medical Sciences, Isfahan, Iran

[3] Department of Genetics and Molecular Biology, School of Medicine, Isfahan University of Medical Sciences, Isfahan, Iran

Therefore, effective therapy for nerve gaps is a coordinated interaction among different components, including the use of supporting cells, the utilization of structural and directional support with NGCs, and the development of an appropriate microenvironment to help cells promote nerve regeneration using necessary factors.

Poly(lactic-co-glycolic acid) (PLGA) is among the excellent biodegradable synthetic polymers used for the fabrication of NGC. PLGA has been adopted in the drug carrier systems due to their favorable mechanical properties and tunable degradation rates (Jahromi et al. 2019; Vaezifar et al. 2015).

In addition, the combination of many physical and biological strategies has been used for fabrication of suitable NGC. Biodegradable electrospun NGCs composed of aligned nanofibers to mimic native nerve ECM are a new class of devices used to guide neurite extensions and axon outgrowth (Sivolella et al. 2014). However, PLGA is hydrophobic and does not have biological recognition sites that can interact with cells to increase cell adhesion and proliferation. Therefore, PLGA should be modified (e.g., with an extracellular matrix such as laminin) in order to increase their hydrophilicity (Huang et al. 2007). In addition, it has been shown that laminin can be stimulate neurite outgrowth in NGC and Schwann cell differentiation (Wu et al. 2017; Zarinfard et al. 2016).

The efficacy of neural synthetic conduit can be decreased by the absence of living cells, inadequate growth factors as biological strategies, and lack of ECM-mimicking biomaterials. So, the presence of cells and neurotrophic factors in NGCs can improve microenvironment for peripheral nerve regeneration (Jahromi et al. 2019).

The application of ADSCs would provide not only large numbers of exogenous seeding cells but also adequate amounts of trophic factors, in situ trans-differentiation, and stromal vascular fraction (Zhang and Rosen 2018). However, traditional stem cell transplantation was usually accompanied with extreme loss and death of transplanted cells, which prevented the therapeutic efficacy for peripheral nerve damage. In this situation, alginate as a hydrogel could support NGC functions due to their hydrophilicity property and protect the injected cells from the immune attack of host immune biosystems (Augst et al. 2006). One approach that has been taken to improve these outcomes is the use of alginate hydrogels that help to retain injected ADSCs and provide a microenvironment that supports cell viability and function without leak out of cells (Galateanu et al. 2012).

Another important factor in nerve tissue engineering is a neurotrophic factor–rich environment that can promote neurogenesis and is essential for nerve regeneration. BDNF is an prominent neurotrophic factor in neural stem cells (NSCs) proliferation, differentiation, and directional migration. Adding exogenous BDNF enhances myelination, whereas the lack of endogenous BDNF decreases the formation of mature myelin (Chan et al. 2001).

Gold nanoparticles (AuNPs) have various biomedical applications such as drug delivery, imaging, and apoptosis stimulus in cancerous cells by the induction of localized hyperthermia (Singh et al. 2018). It has been proven that, in addition to important factors in nerve tissue engineering, AuNPs enhance cell-material interactions in terms of cell adhesion, proliferation, differentiation, stimulate axonal elongation, and sprouting axons (Baranes et al. 2016; Razavi et al. 2019).

Our previous study demonstrated that the coating of BDNF and AuNPs encapsulated in chitosan on nanofibers leads to their continuous release for 7 days, and this could enhance the proliferation and differentiation of adipose-derived stem cells into Schwann cells in vitro (Seyedebrahimi et al. 2020).

These findings can confirm the validity of the proposed strategy in improving the peripheral nerve regeneration in vivo. In this study, we evaluated the effect of controlled BDNF and AuNPs releasing on r-ADSCs suspended in alginate to enhancing peripheral nerve regeneration in a rat sciatic transection model.

Therefore, electrospun PLGA scaffolds were fabricated in different orientation at outer and inner surfaces, random and aligned, respectively. The inner surface of the NGC was coated by laminin that containing encapsulated BDNF and AuNPs in chitosan.

Next, the alginate hydrogel was loaded with r-ADSCs and injected into an NGC that was transplanted to a 10-mm sciatic nerve defect. Eventually, axonal regeneration and motor functional recovery were assessed after 12 weeks.

Materials and Methods

Materials

PLGA (80:20, Mw 50,000-75,000) and chitosan (low molecular weight with a deacetylation degree of > 75%), collagenase type I, 4′,6-diamidino-2-phenylindole (DAPI), laminin, trypsin-ethylenediaminetetraacetic acid (EDTA), anti-neurofilament 160/200, and alginic acid sodium salt were supplied by Sigma-Aldrich (USA). *N*,*N*-dimethylformamide (DMF) and chloroform purchased from Merck (Germany). DMEM/F12, phosphate-buffered saline (PBS), fetal bovine serum (FBS), and penicillin-streptomycin were purchased from Invitrogen. BDNF and AuNPs were obtained from R&D (USA) and US NANO (USA), respectively. Anti-S100, anti-myelin basic protein (anti-MBP), rabbit anti-mouse FITC, and goat anti-mouse Alexa Flour were purchased from Abcam.

Electrospinning of PLGA Nanofibers and Scaffold Characterization

Electrospun scaffolds were fabricated as described in our previous study (Vaezifar et al. 2015), with slight modification. PLGA (80:20, Mw 50,000–75,000) was dissolved in a chloroform: DMF mixture with a volume ratio of 80:20 to obtain a final concentration of 20% (w/v). After stirring for 3 h at room temperature, the polymer solution was loaded into a syringe fitted with a 27 G blunt needle and a high voltage electric field of 21 kV was applied to draw the polymer solution fed at a rate of 250 μl/h into nanofibers over a distance of 15 cm from the needle tip to an aluminum-wrapped rotating drum. To fabricate a nanofibrous scaffold with sufficient isotropic mechanical properties keeping its integrity in vivo, on one hand, and to present aligned nanofibers providing axonal contact guidance, on the other hand, the drum rotation speed was gradually decreased from 2500 to 300 rpm. Therefore, a highly aligned nanofibrous inner surface was formed and, as the drum rotation speed was decreased, fiber orientation gradually diminished. Electrospinning process continued for 9 h, and randomly oriented fibers of outer surface endowed the scaffold with isotropic mechanical properties, while the gradual alteration in fiber orientation could avoid sheet delamination. Finally, scaffolds were opened in the longitudinal direction, removed from the drum, and vacuum dried. Scanning electron microscopy (SEM, Seron Technology AIS 2500, India) was used to observe the morphology of PLGA. For this purpose, electrospun PLGA samples were coated with a thin layer of gold prior to taking SEM images (Brown et al. 2018).

Preparation of BDNF- and AuNPs-Encapsulated Chitosan Nanoparticles in Laminin and Coating on PLGA Sheets

The ionotropic gelation method was used for producing of either AuNPs- or BDNF-encapsulated chitosan nanoparticles (BDNF-CNPs and AuNPs-CNPs) (Seyedebrahimi et al. 2020).

Briefly, 0.1% chitosan solution was prepared and then emulsified with 5 μg/ml BDNF or 50 ppm AuNPs (Lin et al. 2008) for 15 min using a magnetic stirrer. Next, 0.03% TPP of an aqueous solution as cross-linker was added drop wise into the previous solution. The chitosan nanospheres containing BDNF or AuNPs were suspended in 20 μg/ml laminin and then coated on PLGA scaffold at 4 °C for 24 h.

Fabrication of NGCs

PLGA membrane was cut to the appropriate size (14 × 20 mm) and UV sterilized for 2 h. Then, the membrane was coated with chitosan nanospheres encapsulated BDNF or AuNPs mixed in 20 μg/ml laminin. In the next step, the scaffold was rotated 2.5 rounds around Teflon-coated tubes with diameters of 2 mm, while fixing its edges to form a tubular structure like an NGC. All these procedures were performed under sterile conditions.

Isolation and Culture of r-ADSCs

Subcutaneous adipose tissue in the inguinal region was harvested from adult male Wistar rats. The fatty tissue was washed with PBS containing antibiotics (50 ml PBS + 1 ml penicillin/streptomycin) to remove cellular debris, blood cells, and tissue sterilization. The solid fat was cut into pieces. Finally, rat minced fat was transferred into a 15-ml reaction tube and then enzymatic digestion was performed by 0.075% collagenase type I and the mixture was incubated at 37 °C for 30 to 45 min. In the next step, to neutralize the enzyme activity, Dulbecco's modified Eagle's medium containing 10% fetal bovine serum was added into each tube. After centrifugation (1200 rpm for 5 min), the upper fat layer and supernatant were discarded. The remaining cell pellet containing the r-ADSCs was resuspended in DMEM + 10% FBS at 37 °C and 5% CO_2, and the culture medium was changed every 3–4 days (Cornejo et al. 2012).

Surgical Procedures of Animal Subjects

Male Wistar rats ($n = 48$) weighing ~200–250 g were randomly divided into six groups (all animal experiments were approved by the Animal Ethics Committee of Isfahan University of Medical Sciences): (1) control group (Co); (2) PLGA conduit coated by laminin and filled with DMEM/F12 and transplanted in 10 mm sciatic gap (PL); (3) PLGA conduit coated by laminin and filled with 2×10^6 r-ADSCs transplant in 10 mm sciatic gap (PLC); (4) PLGA conduit coated by laminin containing BDNF-chitosan nanoparticles (CNPs) and AuNPs-CNPs, filled with DMEM/F12, and then transplanted in 10 mm sciatic gap (PLGB); (5) PLGA conduit coated by laminin containing BDNF-CNPs and AuNPs-CNPs, filled with 2×10^6 r-ADSCs, and then transplanted in 10 mm sciatic gap (PLGBC); and (6) PLGA conduit coated by laminin containing BDNF-CNPs and AuNPs-CNPs, filled with 2×10^6 r-ADSCs suspend in alginate, and then transplanted in 10 mm sciatic gap (PLGBCA).

Each rat was anesthetized by an intraperitoneal injection of xylazine 10 mg/kg and ketamine 100 mg/kg. The thigh areas on left sides were shaved and then disinfected by povidone-iodine.

The left sciatic nerve was chosen as the examination side in each animal. Afterward, a skin incision was made to expose the sciatic nerve and then the underlying muscles were split in the left thigh.

Next, 10 mm of nerve segment was removed before it branches to fibular, tibial, and sural nerve and coated PLGA

conduit with or without 2×10^6 r-ADSCs injection to the NGC-implanted in different groups.

In the alginate group, 40 μl alginate containing 2×10^6 cells with 20 μl $CaCl_2$ was injected into the NGC. The nerve segment was inserted 2 mm into the ends of the NGC and fixed using 10-0 nylon sutures. Following the implantation, the muscle incision was closed using 7-0 nylon sutures and the skin was closed with 7-0 nylon sutures. Finally, rats were free to access to water and food and housed in a controlled room with 12 h light/dark cycles.

SFI

The motor functional recovery of the peripheral nerve was assessed by sciatic functional index (SFI) during 12 weeks post-operatively. The hind feet of all rats were painted into blue ink. Next, they were allowed to walk in a 50-cm × 10-cm wooden track covered with a white paper. The rats' footprints were used to calculate their SFI by the following formula:

$$\mathrm{SFI} = -38.3\ (\mathrm{EPL}-\mathrm{NPL})/\mathrm{NPL} + 109.5(\mathrm{ETS}-\mathrm{NTS})/\mathrm{NTS} + 13.3(\mathrm{EIT}-\mathrm{NIT})/\mathrm{NIT}-8.8$$

The print length (PL) is the distance from the heel to the third toe, the toe spread (TS) is the distance from the first to the fifth toe, and the intermediary toe spread (IT) is the distance from the second to the fourth toe. All measurements were calculated from the normal (N) and the experimental (E) sides. SFI ranged from 0 for normal nerve function till − 100 for complete injury (Bain et al. 1989).

Muscle Mass

Twelve weeks post-operatively, the gastrocnemius muscle of experiment and normal legs in all rats were dissected and immediately weighed (while still wet) using an electronic balance (A&D Weighing EK-3000I Portable Balance, 3000g Capacity). The recovery ratio and muscle atrophy of the gastrocnemius were calculated by the muscle wet weight of the injured limb/the weight of the contralateral one × 100% (Li et al. 2018).

Histological Examination

To evaluate the physiological status of nerve fiber, myelin sheath, and muscle recovery at 12 weeks after NGC implantation, the operated nerve and muscle specimens were stained and analyzed. After sacrificing an animal, the gastrocnemius of both the limbs and the nerve-implanted conduits was harvested for histological examination. The central segment nerves and muscles were fixed in 10% neutral buffered formalin for 48 h. The samples were then dehydrated through a graded ethanol series, cleared in xylene, and cut into 5-μm-thick sections after paraffin embedding. The transverse sections of the gastrocnemius muscle were stained with Masson trichrome and observed using a lighted microscope. The mean diameter of the muscle fibers was calculated using Digimizer software an image analysis system.

Nerve samples were stained with toluidine blue to label the myelin sheath and evaluated under light microscopy. The degree of myelination was estimated by G-ratio (the axon-to-fiber diameter ratio). To quantify the mean number of a myelinated axon, nine images were randomly captured at × 400 magnification for each group and 5 fields of all images were counted to obtain the mean numbers of myelinated nerve fibers. The average diameter of the sciatic regenerated nerve fibers, axon, and myelin and the mean number of myelinated axons were calculated using Digimizer software.

Immunohistochemistry

Twelve weeks after surgery, the regenerated sciatic nerves were removed from rats in each group. The immunohistochemistry (IHC) staining was performed to detect specific Schwann, myelin, and growing axon markers using S-100, MBP, and NF-200, respectively. Briefly, nerve animals were fixated with 4% paraformaldehyde (PFA) at 4 °C for 6 h and then paraffin embedded cut into 3-μm-thick sections.

For double immunostaining analysis of NF200 and S100 or NF200 and MBP in the sections, antigen unmasking was performed using a 10 mM sodium citrate buffer with pH = 6.0, at 90 °C for 10 min. Afterward, it was incubated for 30 min in blocking serum (10% normal goat serum to cover unspecific binding) and then incubated overnight at 4 °C with the following diluted primary antibodies: anti-S-100 β (1:500), anti-myelin basic protein (anti-MBP) (1:500), and anti-neurofilament 200 (NF-200) antibody (1:100). After washing with PBS, the sections were incubated with secondary antibodies: rabbit anti-mouse FITC (1:500) and goat anti-mouse Alexa Flour (1:1000).

The cell nuclei were stained with DAPI (1:1000). The stained sections were studied under a fluorescent microscope (Olympus BX51, Japan). For each section, three images were captured randomly with a digital camera at × 100 magnification. Then, the total area of the images was measured for intensity with ImageJ software. Finally, the percentage of positive intensity of NF200, S100, and MBP staining were assessed and compared with the control group.

TEM

The middle segment of the regenerated nerve was cut and fixed in 2.5% glutaraldehyde. Subsequently, the specimen was fixated in 1% osmium tetroxide, dehydration in graded ethanol, and then embedded in epoxy resin. Ultrathin sections of 50 nm thickness were prepared using an ultramicrotome,

collected on copper grids, contrasted in lead citrate, and examined by TEM. Next, the morphology of neural fibers was compared for axon and myelin diameter in different groups.

Real-time Reverse Transcription Polymerase Chain Reaction

Quantitative real-time RT-PCR was conducted to detect the S100, MBP, GFAP, and Nestin mRNA levels in the NGC of the regenerated sciatic nerve. The expression levels were normalized against the reference gene, β-actin as the control housekeeping gene, and the relative gene expression was analyzed.

Total RNA was isolated from the nerve tissues using Total RNA Prep Kit (BIOFACT). The RNA was reverse transcribed using BioFact™ 5× RT Pre-Mix cDNA Synthesis Kit (BIOFACT) with oligo dT primers. The real-time PCR was performed using BioFact™ 2× Real-time PCR Master Mix kit (BIOFACT) and the StepOne Plus™ quantitative Real-time PCR Detection System (Applied Biosystems). The primers were purchased from metabion (Germany). The detailed sequences of primers for each gene are displayed in Table 1.

Statistical Analysis

Descriptive analysis was used for all of the results, and the data of the behavioral test (comparing groups at different times) and a quantitative analysis of immunohistochemical, histology, and real-time RT-PCR were statistically analyzed by the one-way analysis of variance (one-way ANOVA) using SPSS 22 statistical software, and a post hoc analysis for comparing the mean of examined different variables between experimental groups was performed according to Tukey's method. Also, data related to immunohistochemical and the muscle wet weight are presented as percentages of control. Data are described as mean ± standard error (SE). The significant difference mean between experimental groups was determined at $p < 0.05$, whereas $p < 0.01$ and $p < 0.001$.

Table 1 The list of primer sequences of *S100* (Schwann cell marker), *Nestin* (marker of neural progenitor cells), *Gfap* (glial fibrillary acidic protein), *Mbp* (myelin basic protein), and *β-actin* (as the control housekeeping gene) for real-time RT-PCR analysis

Gene	Primer (forward (top) reverse (bottom))
S100	5′-ATAGCACCTCCGTTGGACAG-3′
	5′-TCGTTTGCACAGAGGACAAG-3′
Nestin	5′-CCGGGTCAAGACGCTAGAAGA-3′
	5′-CTCCAGCTCTTCCGCAAGGTTGT-3′
Gfap	5′-CTCCTATGCCTCCTCCGAGACGAT-3′
	5′-GCTCGCTGGCCCGAGTCTCTT-3′
Mbp	5′-CACAGAAGAGACCCTCACAGCGAC-3′
	5′-CCGCTAAAGAAGCGCCCGATGGA-3′
β-actin	5′-TGTCCACCTTCCAGCAGATGT-3′
	5′-GCTCAGTAACAGTCCGCCTAGA-3′

Results

Characterization of the NGC and Transplanted Cells

The PLGA conduit was fabricated by electrospinning method, and the structure of the scaffold was observed by SEM. The fabrication of two surface of nanofiber scaffold was verified by SEM (Fig. 1a). The outer surface consisted of random arranged PLGA fibers (Fig. 1a (a)), while the inner surface of the membrane contained align fibers (Fig. 1a (b)). The average thickness of the PLGA sheets was 73.8 ± 2.05 μm. But the mean thickness of laminin-coated scaffolds with or without BDNF/AuNP-encapsulated chitosan nanoparticles was calculated 77.8 ± 2.05 μm. The PLGA scaffold (14 × 20 mm) was rolled around 2-mm diameter Teflon mandrel, and edges of the roll were secured together to form PLGA conduit in ~ 1.4 cm in length and 2 mm in diameter (Fig. 1 b and c). The size of PLGA conduit is suitable for bridging a 1-cm gap of the sciatic nerve in the rat.

After 3–4 passages, the r-ADSCs had fibroblast-like form, appeared regular, and were larger in size (Fig. 1d).

Animal Model and NGC

At 12 weeks after surgery (Fig. 1e), NGC implantation was successful in all experimental groups (Fig. 1f). All experimental rats survived without any infections or complications and surgical wounds restored well. Twelve weeks after the surgery, surgical areas were re-exposed and it was observed that the sciatic NGC bridged the defects of the NGC in all groups. Moreover, muscle tissues and mild adhesion to surrounding muscles with no dislocation were observed in all groups. The new blood capillaries were observed on the NGC surface. No obvious swelling or scars were observed on the nerve implantation surface.

SFI Outcome

Motor functional recovery after sciatic nerve injury was evaluated using the SFI as a reliable method to assess the recovery of innervation of foot muscles and nerve regeneration at 1, 2, 4, 8, and 12 weeks post-implantation. The mean of SFI value was not significantly different among the five implanted NGC groups before 2 weeks; however, there was an ascending time-dependent trend. From week 8, the mean of SFI value in all of the implanted groups was significantly different from each other and the control group ($p < 0.05$). Moreover, the superior recovery in the PLGBCA group continued during 4, 8, and

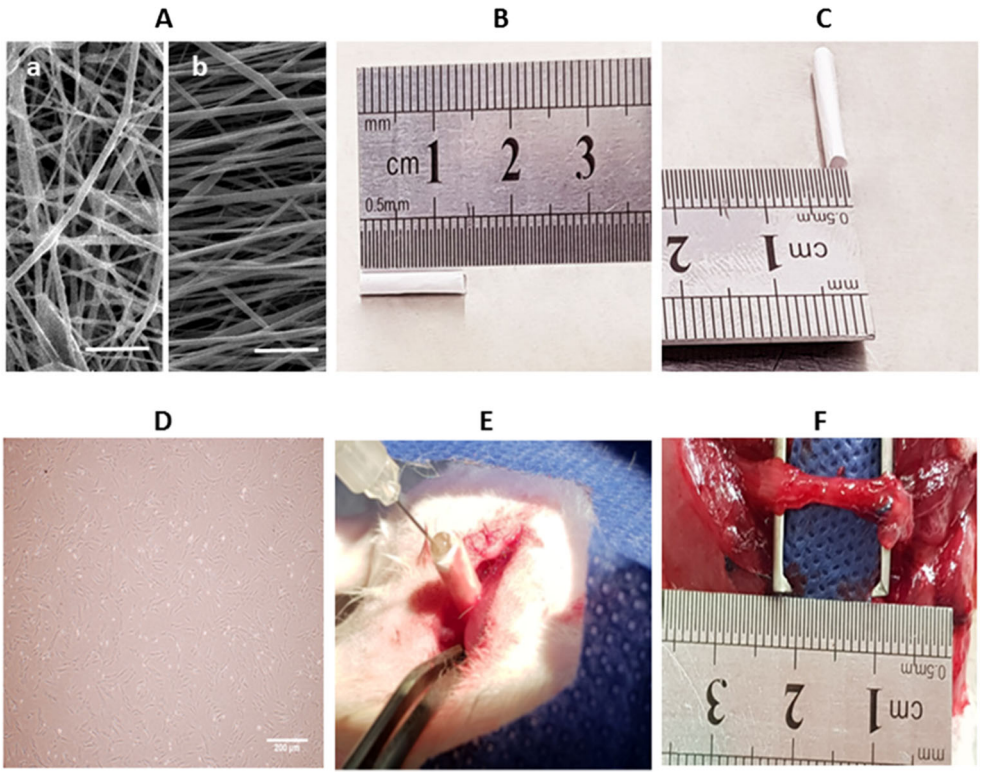

Fig. 1 Scanning electron microscope images of the PLGA nerve conduit (scale bar is 5 μm) (**a**), the outer surface of the membrane contained random fibers (**a** (a)), while the inner surface consisted of aligning arranged PLGA fibers (**a** (b)). The length and diameter of nerve conduit (**b**, **c**); Morphology of r-ADSCs (scale bars = 200 μm) (**d**). Conduit implanted surgery (**e**). Conduit implanted in 10 mm rat sciatic nerve gap 12-week post-operative (**f**)

12 weeks (Fig. 2a and b). The motor function in the PLGBC and PLGBCA rats was superior to the PLGB, PLC, and PL animals but inferior to the normal control rats. Moreover, the superior recovery in the PLGBCA group continued through week 12.

Histological Analyses of the Gastrocnemius Muscle

After peripheral nerve injury, Masson's trichrome staining was used to assess the regrowth of target muscles (Fig. 3a–f). The atrophy can be gradually relieved in animals that received one of the artificial implants, which contained encapsulated r-ADSCs in alginate, BDNF, and AuNPs (Fig. 3a–f). The mean of muscle fibers diameter in the PLGBCA group was significantly higher than other implanted groups at 12 weeks ($p < 0.001$) and was comparable with the control group. The results demonstrated that the recovery from atrophy and regain muscle mass after undergoing regenerating nerve reinnervation of the PL group was slightly lower than that in the other implanted groups (13.2 ± 0.36) (Table 2).

Wet Muscle Weight of the Gastrocnemius Muscle

The gastrocnemius muscle atrophy is a secondary effect after sciatic nerve defect due to the lack of activity that regains innervation after nerve regeneration. The atrophy leads to muscle weight loss, smaller muscle fibers, and a high amount of collagen fibers, which continue until the muscle is fully reinnervated. The mean gastrocnemius muscle weight of the PLGBCA group showed significant difference with other implanted groups at 12 weeks after implantation ($p < 0.001$) (Fig. 3g and h). Also, in PLC, PLGB, and PLGBC, muscle atrophy was significantly lower compared with the PL group ($p < 0.001$).

Nerve Histomorphometry and Transmission Electron Microscopy Study

Toluidine Blue staining was used to visualize regenerated nerve morphology and assess myelin sheath thickness, the axon diameter, nerve fibers, and the degree of myelin formation which was calculated by the axon-to-fiber diameter ratio (G-ratio) and counting the average number of myelinated axons (Fig. 4a–f; Table 2). Nerve regeneration was examined in the transverse sections of the implanted NGC with regenerated myelinated nerve fibers in different numbers and sizes for normal control and implanted nerve groups (Fig. 4a–f).

The myelinated nerve fibers in the control group were depicted as the most regular arrangement. However, the myelinated nerve fibers in the PL group were arranged in a relatively sparse and irregular manner. Also, the arrangement of the axons in PLBG, PLGBC, and PLGBCA groups was the most regular compared with the PL and PLC treatment groups.

A large number of connective tissue and new blood vessels were found around the nerve fiber in PL, PLC, and PLGB

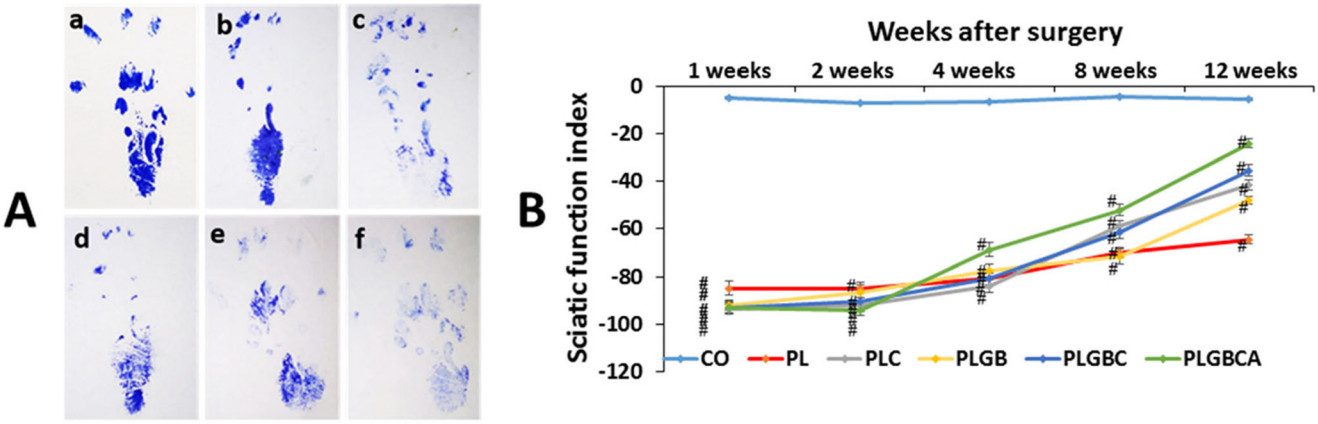

Fig. 2 The representative operative left footprints in sciatic functional index (SFI) (**a**) in the control group (a), PL group (b), PLC group (c), PLGB group (d), PLGBC group (e), and PLGBCA (f) at 12 weeks post-operative. The SFI of six groups at 1, 2, 4, 8, and 12 weeks after surgery (**b**) ($^{\#}p < 0.001$, conduit-implanted group compared with normal control group). Co (control), P (PLGA), L (laminin), G (AuNPs), B (BDNF), C (Cell), A (alginate)

groups in comparison with the normal control group. The average number of myelinated axons in PLGBCA group was significantly increased compared with the PL and PLGBC groups ($p < 0.05$). In addition, the mean diameter of myelinated axons and nerve fiber, the G-ratio, and the thickness of myelin sheath of the NGC-implanted groups were found to be statistically no significant difference in all groups ($p > 0.05$). In this regard, PLGBCA and PLGBC groups were comparable with the normal control group. However, there is still a significant difference between the NGC-implanted groups and normal control group in the number myelinated axons, the diameter of axon myelinated, and the fiber diameters ($p < 0.05$) (Table 2).

The result of toluidine blue staining for the regenerated nerves was confirmed by transmission electron microscopy (TEM) images (Fig. 4g–l).

Immunohistochemical Analysis of Regenerated Nerves

The immunohistochemical assessment was carried out by double NF200/S100 and NF200/MBP staining shown in Fig. 5, respectively. First, we evaluated nerve regeneration by evaluating of S100, MBP, and NF200 markers in longitudinal tissue sections of the middle portion in NGCs implanted 12 weeks after the surgery.

All groups had significant intense staining of NF200, MBP, and S100 positive cells in the NGC-implanted region ($p < 0.001$). In comparison with PL group, the intensity of MBP marker was significantly lower in the PLC, PLGB, PLGBC, and PLGBCA groups 12 weeks after surgery ($P < 0.001$). The defect sciatic nerve of rats that implanted with PLGBCA contained significantly NF200 and S100 intensity area compared with the control and other implanted groups ($p < 0.001$) (Fig. 6a–c).

Quantitative Real-time PCR

In order to assess the effect of NGC contain nanoparticles and r-ADSCs in nerve regeneration, the levels of specific Schwann cell markers (S100β), glial marker (GFAP), myelination ability (MBP), and neural precursor marker

Table 2 Quantified diameter of muscle fiber, myelinated axon, nerve fiber, G-ratio, average number of myelinated axon and thickness of myelin sheath in Co (control), P (PLGA), L (laminin), G (AuNPs), B (BDNF), C (cell), and A (alginate) groups. Data are mean ± standard error

Groups	Muscle fibers diameter (μm)	Myelinated axons diameter (μm)	Nerve fibers diameter (μm)	Myelin sheath thickness (μm)	Average number of myelinated axon (per field)	G-ratio
Co	23.6 ± 2.3	4.5 ± 0.09	8.35 ± 0.37	3.78 ± 0.32	27.7 ± 0.88	0.54 ± 0.02
PL	13.02 ± 0.36***	2.03 ± 0.15***	4.76 ± 0.25***	2.72 ± 0.24	14.2 ± 1.05***	0.42 ± 0.02*
PLC	14.4 ± 0.67***	2.7 ± 0.21***	6.11 ± 0.34**	3.36 ± 0.20	17.6 ± 0.60***	0.45 ± 0.02
PLGB	13.5 ± 0.92***	2.4 ± 0.28***	5.76 ± 0.73**	3.36 ± 0.52	17.6 ± 0.75***	0.49 ± 0.04
PLGBC	16.5 ± 0.71**	2.9 ± 0.34***	6.27 ± 0.54*	3.35 ± 0.24	15.4 ± 1.5***	0.46 ± 0.02
PLGBCA	19.0 ± 0.90*	2.9 ± 0.06***	6.45 ± 0.31*	3.52 ± 0.31	22.1 ± 1.1*	0.45 ± 0.02

*$p < 0.05$; **$p < 0.01$; ***$p < 0.001$ significant values of conduit implanted group compared with normal control group

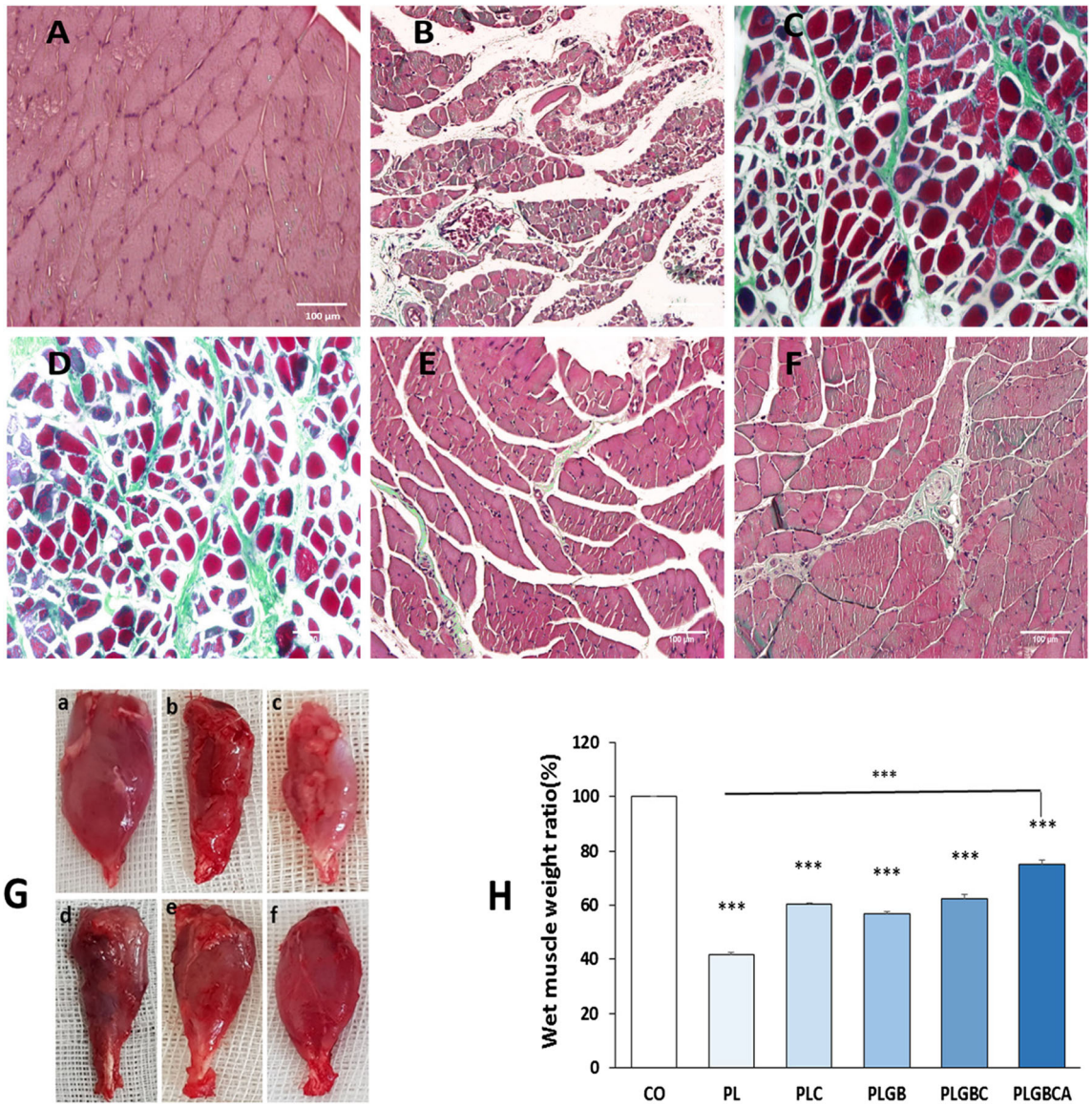

Fig. 3 Representative images of transverse sectioned gastrocnemius muscle following Masson trichrome staining (**a–f**); The control group (**a**), PL group (**b**), PLC group (**c**), PLGB group (**d**), PLGBC group (**e**), and PLGBCA (**f**) at 12 weeks post-operative (scale bars = 100 μm). Photographs and determination mean ratios of gastrocnemius muscles weight (%) at 12 weeks post-operative (**g**, **h**). The control group (a), PL group (b), PLC group (c), PLGB group (d), PLGBC group (e), and PLGBCA (f) ($p < 0.001$ ***, conduit implanted group compared with normal control group). Co (control), P (PLGA), L (laminin), G (AuNPs), B (BDNF), C (cell), A (alginate)

(Nestin) were evaluated through real- time RT-PCR technique 12 weeks after the surgery (Fig. 6d–g).

The level of GFAP was significantly downregulated in the PLGB group compared with the control group ($p < 0.05$), but there was no significant difference in the expression of this gene between PL, PLC, PLGBC, and PLGBCA groups with the control group.

Despite the expression level of S100 by Schwann cells, no significant difference was observed among the NGC-implanted groups and control group ($p > 0.05$). However, there was a significant difference in the expression of S100 gene between PLGBCA group and other NGC-implanted groups ($p < 0.05$), except with the PLC group (Fig. 6e).

Compared with the control group, the expression of MBP marker was significantly lower in the PL, PLGB, and PLGBC groups 12 weeks after the operation ($p < 0.05$). However, we observed that the presence of alginate also could increase in the expression level of MBP in PLGBCA group (1.24 ± 0.34) compared with the control group (1 ± 0.1), but it was not significant ($p > 0.05$) (Fig. 6f). Also, the level of Nestin expression in nerve-implanted conduit containing alginate (PLGBCA) group was significantly upregulated compared with control and other implanted NGC groups ($p < 0.001$).

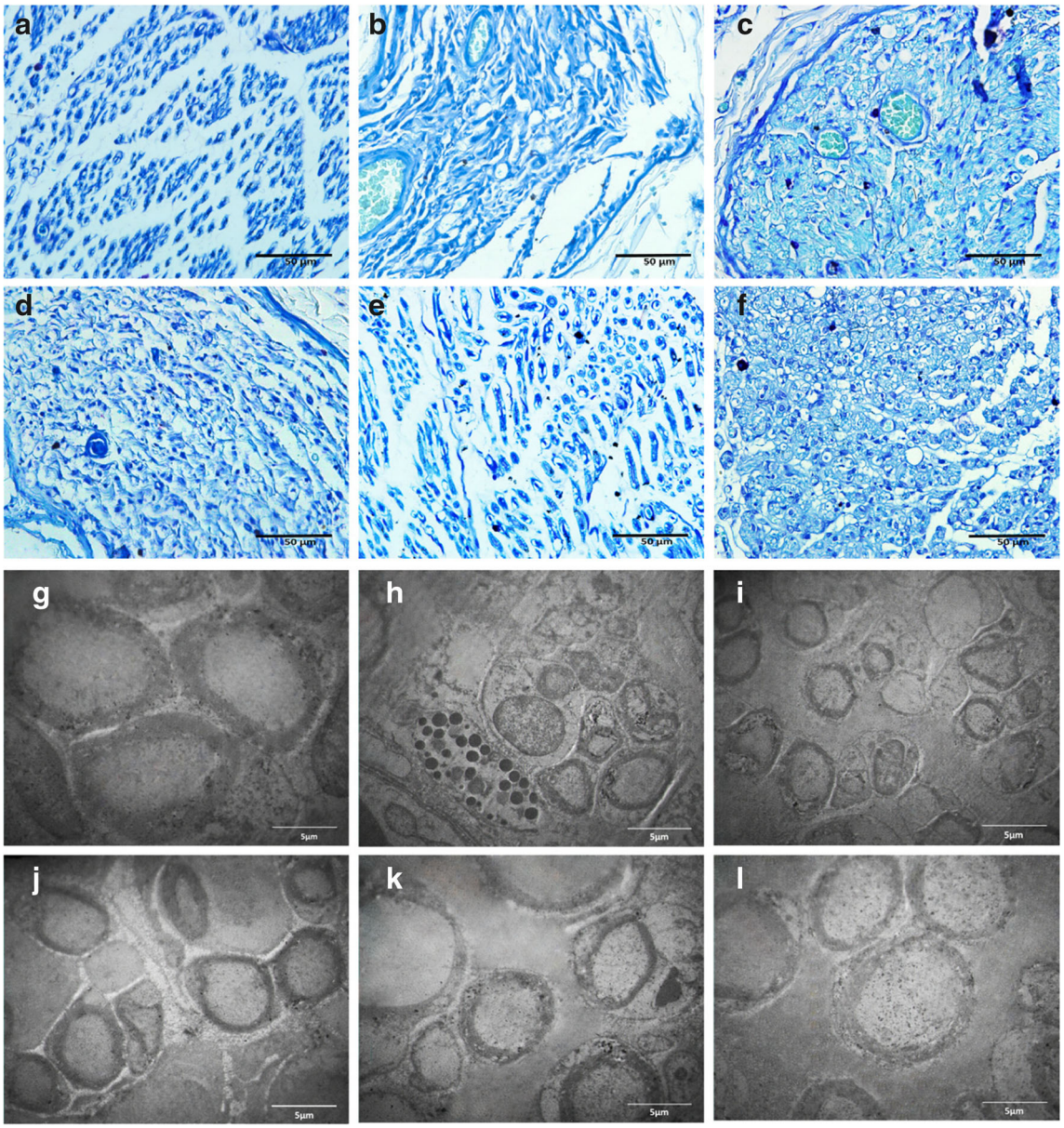

Fig. 4 Histology of regenerated axons for toluidine blue staining in the regenerated nerve under light microscopy at 12 weeks post-operative (scale bars = 50 μm) (**a**–**f**); TEM micrographs of repaired axons and myelin sheath in different groups at 12 weeks post-operative (scale bars = 5 μm) (**g**–**l**); in the control group (**a**, **g**), PL group (**b**, **h**), PLC group (**c**, **i**), PLGB group (**d**, **j**), PLGBC group (**e**, **k**), and PLGBCA group (**f**, **l**); P (PLGA), L (laminin), G (AuNPs), B (BDNF), C (cell), A (alginate)

Discussion

In this study, the effect of AuNPs- and BDNF-encapsulated chitosan nanoparticle in laminin-coated nanofiber PLGA conduit with or without r-ADSCs suspend in alginate to promoting axonal regeneration after sciatic nerve injury is evaluated.

The nanofiber scaffolds consisted of aligned inner surface of PLGA fibers that coated with laminin for directional guidance, containing AuNPs and BDNF encapsulated in chitosan nanoparticle filled with r-ADSCs for promoting the sciatic nerve regeneration. In comparison, the outer surface of the NGC was prepared with randomly oriented PLGA nanofibers to strengthen the weak mechanical property of aligned nanofibers.

Previously, we have demonstrated that controlled release of BDNF and AuNPs by chitosan nanoparticles could significantly promote the viability, proliferation, and differentiation of ADSCs in vitro. In addition, BDNF was released from nanofibers about 74 ± 2.42% after 7 days while the release rate of AuNPs was slower (47.24 ± 1.78%). Also, 20 μg/ml laminin peptide–coated PLGA nanofibers have no cytotoxic effect on ADSCs viability and could promote the proliferation of ADSCs in vitro. Also, in previous study, the effect of functionalized PLGA scaffold with laminin and nanoparticles

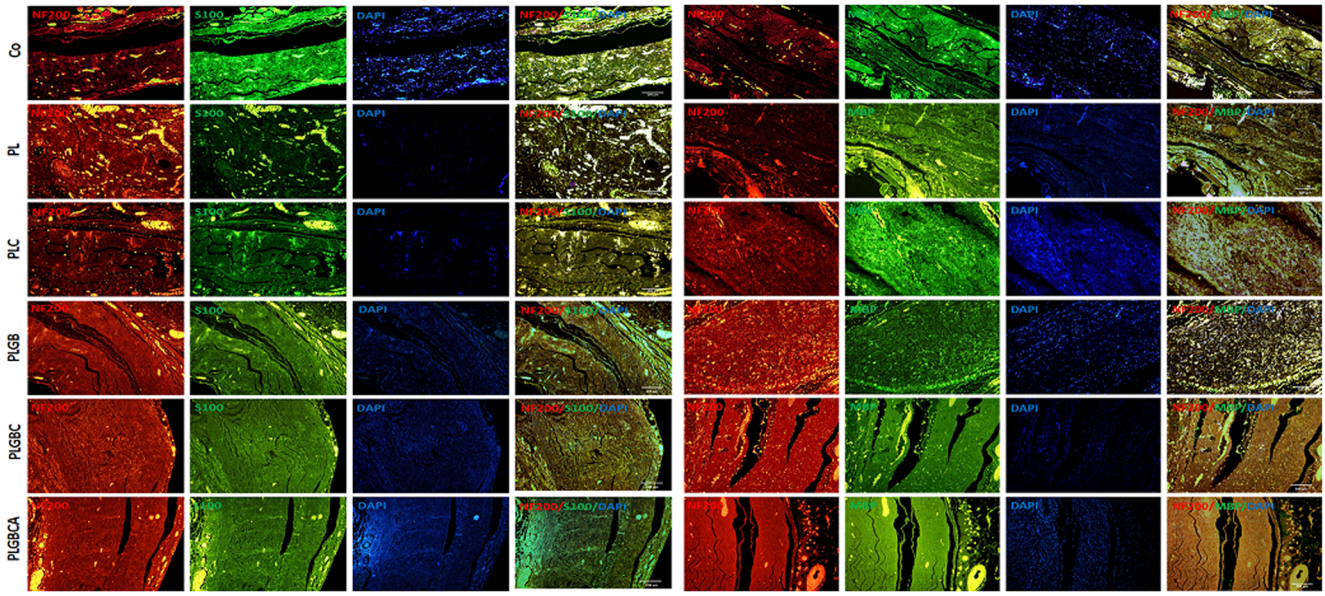

Fig. 5 Double-immunohistochemical staining of regenerated nerve longitudinal sections with NF-200/S-100 and NF-200/MBP in each group; neurofilaments were labeled with NF-200, which exhibits a red color. Schwann cells were labeled with S-100 appears as green (scale bars = 200 μm). Cells were labeled with MBP, which appears as green (scale bars = 200 μm); Co (control), P (PLGA), L (laminin), G (AuNPs), B (BDNF), C (cell), A (alginate)

showed that the presence of laminin and constant release of BDNF and AuNPs improve the differentiation of adipose-derived stem cells into Schwann and myelinating ability (Seyedebrahimi et al. 2020). Thus, in this study, we purposed coating exogenous encapsulated BDNF and AuNPs on the surface of electrospun PLGA nerve conduits to promoting peripheral nerve regeneration after injury.

In the current study, immunohistochemical staining of nerves longitudinal sections revealed different degrees of nerve regeneration, while the nerve growth pathway was proximal to distal in all groups. This may be due to the presence of longitudinally aligned nanofibers on the inner surface of the NGC to mimicking the native peripheral nerve's fascicular architecture. Overall, aligned nanofibers not only provide effective physical guidance but also foster accelerated nerve repair by supporting axonal path finding during regrowth (Dinis et al. 2013).

Our finding is constant with the results of Schuh et al. (2014), who showed that highly aligned electrospun fibrin-PLGA fibers promote the differentiate and proliferation of r-ASCs to Schwann cell–like cells (SCLs) (Schuh et al. 2014).

We chose PLGA scaffold as a biodegradable NGC for guiding nerve repair. The biodegradable NGC has the advantage of avoiding a secondary surgery of NGC removal after nerve regeneration. Also, PLGA is one of the few biomaterials approved by the US Food and Drug Administration (FDA) for experimental and clinical application. Also, PLGA has broad applications in drug delivery and tissue engineering, especially in neural tissue engineering (Jahromi et al. 2019) .

To mimic the in vivo condition, different factors such as stem cells, growth factor, and other stimulating particles have been included in the NGCs, and observations indicate that they have a positive effect on nerve regeneration.

It has been shown that ADSCs have the potential of inhibit neuronal cell death and muscle atrophy after nerve injury (Zhang and Rosen 2018). In addition, Schwann-like cell induced from ADSCs can decline the level of pro-apoptotic Bax marker and caspase-3 expression as well as increase anti-apoptotic Bcl-2 expression in the NGC. Therefore, the anti-apoptotic effect of ADSCs in NGC may be through of BDNF, NGF, and GDNF factors releasing and neuroprotective effect of ADSCs via IGF-1 and BDNF secretions (Reid et al. 2011; Wei et al. 2009).

Hydrogels such as alginate can serve as biocompatible and FDA-approved drugs that might be used as a hydrogel inside the NGC for clinic application of nerve regeneration because alginate does not stimulate the host immune response (Hashimoto et al. 2002). Alginate as a natural polysaccharide has several advantages such as injectability, biodegradability, and porosity (Galateanu et al. 2012). In addition, it is rapidly cross-linked in the presence of divalent cations such as calcium gluconate (Ma and Elisseeff 2005). Based on our findings, the presence of hydrogel alginate inside the NGC not only leads to stability of the PLGA conduit but also facilitates the suturing procedure by preventing collapsing of the NGC.

In the current study, we used BDNF and AuNPs for promoting peripheral nerve regeneration. Exogenous BDNF can promote outgrowth of axon into the distal nerve stumps as

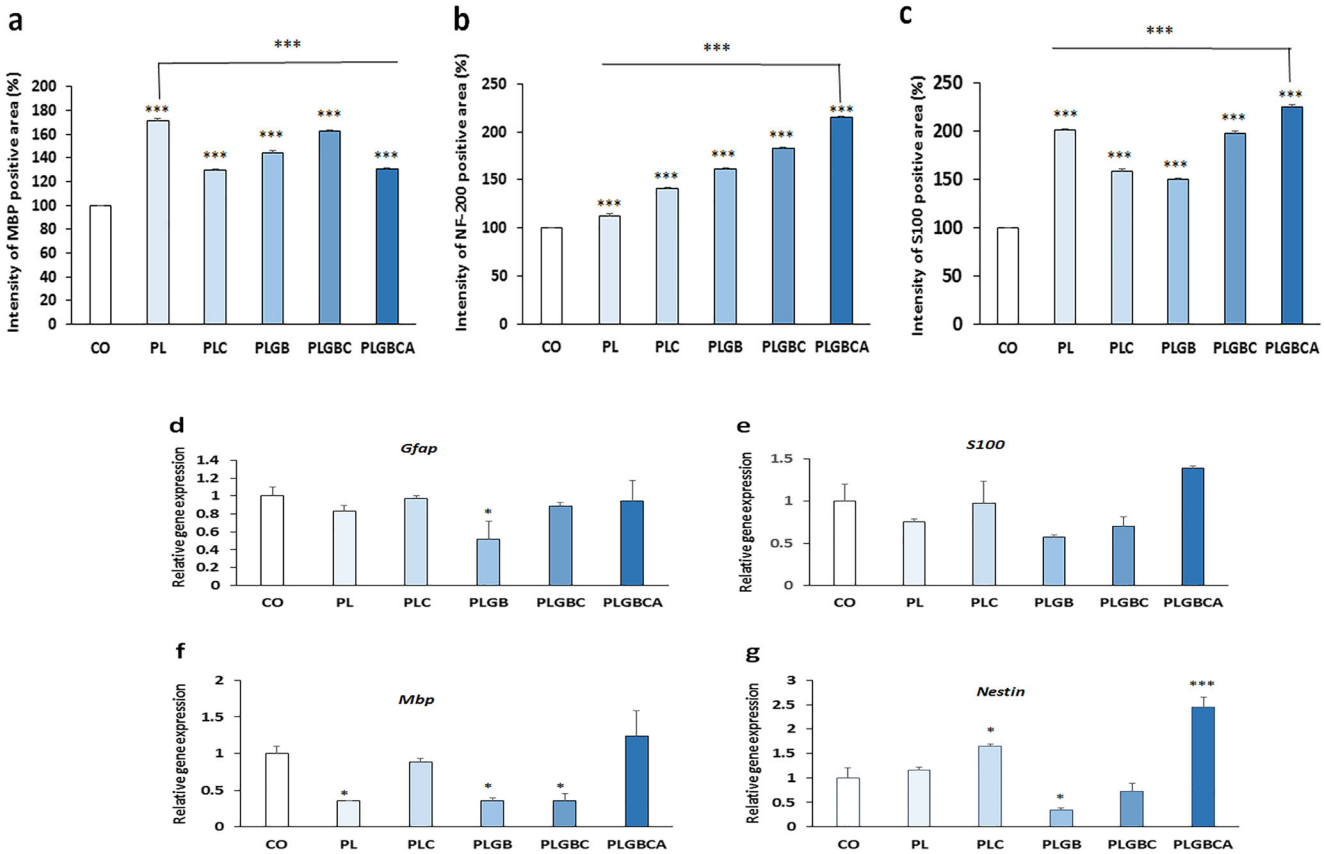

Fig. 6 A comparison intensity value for MBP, NF200, and S100 in different groups is shown in **a**–**c**. The level of GFAP, S100, MBP and Nestin, expression in different groups evaluated by real-time RT-PCR (**d**–**g**), Co (control), P (PLGA), L (laminin), G (AuNPs), B (BDNF), C (cell), A (alginate) (*$p < 0.05$, ***$p < 0.001$ conduit implanted group compared with normal control group)

well as endogenous source of this factors from Schwann cells (Boyd and Gordon 2003).

However, several neurotrophic factors, such as nerve growth factor, hepatocyte growth factor, vascular endothelial growth factor, glial-derived neurotrophic factor (GDNF), brain-derived neurotrophic factor (BDNF), and insulin-like growth factor (IGF), play an essential role in neural survival by protecting neurons from death and finally increasing the potential for axonal repair and treatment of neuropathies after neural injury (Ismail et al. 2020; Jiang et al. 2020; Li et al. 2020). On the other hand, researchers have found that treatment with FGF2 can induce production of different growth factors in vitro and in vivo (Jiang et al. 2020). Following sciatic nerve injury, a transient increase in the expression of BDNF is found in motoneurons. Thus, the rapid upregulation of BDNF makes it likely that BDNF is the main neurotrophin that mediates early motor neuron response to nerve injury. It has been shown that BDNF application to damaged axons increases the number of actin waves (transport of actin filaments and associated proteins toward the growth cone) per hour.

The importance of a single nucleotide polymorphism in the BDNF gene, Val66Met, which is present in 30% of the human population and may hinder the efficacy of these treatments in promoting regeneration after injury is considered (Katsarou et al. 2017; McGregor and English 2019; Siokas et al. 2019). Thus, genetic factors may influence outcomes and the application of exogenous BDNF can enhance axonal regeneration, functional recovery, and decreases synaptic stripping specially among BDNF genetic mutations of human populations (McGregor and English 2019).

Also, it has been shown that AuNPs modulate neural activity, promote call adhesion and proliferation, and stimulate branching of axons (Baranes et al. 2016).

But the administration of exogenous growth factors or AuNPs in environment would result in uncontrolled release and quickly degradation due to deactivation by enzymes and other physical-chemical effectors in vitro and in vivo (Zhuang et al. 2016). Therefore, we used chitosan, as a protective and effective polymer, which provides controlled release of the BDNF and AuNPs for differentiation of ADSCs in NGC.

In the present study, we focus on the effect of controlled release of neurotrophic factor to enhance peripheral nerve regeneration. Twelve weeks after left sciatic nerve transection and implantation of NGC in different groups, a macroscopic examination was performed to assess the degradation

conditions of the NGC and the presence of nerve filaments inside the NGC reconnecting between the two nerve stumps. This qualitative analysis demonstrated that all rats of different groups had NGCs with appropriate degradation. However, macroscopic observation was confirmed by histological analysis.

Jing et al. showed that PLGA conduit with aligned fibers provided strong orientation guidance and desirable degradation 12 weeks post-implantation (Jing et al. 2018).

The behavioral test is essential for the quantitative analysis of motor recovery during the neural tissue regeneration. In this study, we investigated motor nerve recovery via the SFI test.

The motor function in the PLGBC and PLGBCA rats was superior to the PLGB, PLC, and PL animals but inferior to the normal control rats. In addition, the mean SFI values in all the implanted groups were significantly different from each other and the control group ($p < 0.05$).

Our findings in SFI test demonstrated that the BDNF and AuNPs may be delivered locally in the implanted NGC to influence of chitosan degradation, and subsequent direct transfer of alginate could enhance differentiation and proliferation of r-ADSCs and finally increase significant axon growth in implanted site.

Shanbhag et al. demonstrated that alginate acts as a multifunctional scaffold for CNS regeneration and delivery of neurotrophic factors, such as the brain-derived neurotrophic factor to influence the survival, migration, and differentiation of neural progenitor cells (NPCs) seeded on its surface (Shanbhag et al. 2010).

Overall, we observed beneficial effects on gait analysis in PLGBCA compared with other NGCs. This treatment resulted in a significant increase in axon regeneration and reinnervation of the gastrocnemius muscle in different methods, which suggests that alginate could be protect and enhance effect of neural promoting factors in nerve regeneration and functional recovery.

Although, the gold standard for measuring of functional recovery following rat sciatic nerve injury is the SFI. However, the application of additional tools such as automated recording of motor activity of rats using Photobeams Activity System is recommended (Dziwenka et al. 2020; Wang et al. 2018).

The histological evaluations showed that in PLGBCA group and then other implanted groups containing r-ADSCs, AuNPs, and BDNF, the myelinated axon and neural fiber had larger diameters; however, the thickness of the myelin sheath and the G-ratio was not significantly different between the normal control and other implanted groups ($p > 0.05$), except in PL group where G-ratio had a significant difference with control group ($p < 0.05$). Our results are consistent with previously published reports, which demonstrated that alginate gel has excellent biocompatibility for Schwann cell migration and regenerating axon outgrowth. Also, it was reported that the regenerated fibers in alginate group became as large in diameter as those in the normal sciatic nerve (Hashimoto et al. 2002).

In addition, the number of myelinated axons in the alginate group was close to the control. As a result, in the groups containing the AuNPs and the BDNF, there was a higher number of axons, suggesting that the synergistically encapsulated two nanoparticles can differentiate r-ADSCs to Schwann cells and ultimately lead to repair of the damaged nerve.

The presence of alginate probably provides microenvironment that protects the r-ADSCs from external factors (Galateanu et al. 2012). Moreover, it provides an appropriate environment for distributing AuNPs and BDNF delivery result supporting differentiation, survival, and proliferation of r-ADSCs (Keshavarz et al. 2018; Shanbhag et al. 2010).

Although, there is still insufficient knowledge about the consequences of nanomaterials effects on intracellular pathways of in vivo, but the results showed that the presence of AuNPs in the NGCs was able to support regeneration of the sciatic nerve injury (Paviolo and Stoddart 2017).

The available literature reports about cellular toxicity of a AuNPs, both in vitro and in vivo, vary widely in their conclusions (Ostrowski et al. 2009).

Since the AuNPs are considered as a synthetic exogenous factor, it has been shown that synthetic materials such as benomyl can be neurotoxic potentially via evaluating oxidative stress and cytotoxicity and, finally, induce cell apoptosis and death (Kara et al. 2020).

It has been implied that oxidative stress seems to be one of the molecular mechanisms; available scientific information is scarce, especially those that related to the nervous system. Gurunathan et al. showed that the toxic effect of retinoic acid appeared to be reduced in cells treated with retinoic acid in the presence of AuNPs, which was coincident with the increased levels of anti-oxidant markers including glutathione peroxidases, thioredoxin, glutathione disulfide, catalase, glutathione, and superoxide dismutase. Simultaneously, AuNPs ameliorated the apoptotic response by decreasing the mRNA expression of *p21*, *p53*, *Bak*, *Bax*, *caspase-3*, and *caspase-9* and increasing the expressions of *Bcl-Xl* and *Bcl-2*. Therefore, they suggested that AuNPs could be appropriate therapeutic agents for the treatment of oxidative stress–related diseases such as diabetes, atherosclerosis, rheumatoid arthritis, cancer, and neurodegenerative diseases (Gurunathan and Kim 2018).

In addition, Shukla et al. demonstrated that the cytotoxicity of gold nanoparticles has been correlated with a detailed study of their endocytosis uptake and their findings by the assessment of cytotoxicity and immunogenic effects of gold nanoparticles on RAW264.7 macrophage cells found that AuNPs are not cytotoxic, reduce nitrite species and reactive oxygen production, and do not elicit secretion of proinflammatory cytokines IL1-β and TNF-α, making them proper candidates for nanomedicine (Shukla et al. 2005).

However, many reports indicated that AuNPs are nontoxic, in the study of Dobrovolskaia et al., AuNPs of diameter 30 and 50 nm have been shown to be "blood compatible" and did not induce any detectable platelet aggregation, immune response, or change in plasma coagulation time (Dobrovolskaia et al. 2009).

In nerve tissue–engineered delivery systems, the release of exciting and growth factors plays a crucial role for axonal repair (Böcker et al. 2019). In our previous study, we showed that the BDNF was constant released of chitosan/TPP particles during the 7 days (Seyedebrahimi et al. 2019) and BDNF may affect on ADSCs differentiation into Schwann-like cells phenotype during this time, new differentiated SCs, lead to express a range of growth factors in environment for stimulating neurite outgrowth (Georgiou et al. 2015). Additionally, the encapsulation of ADSCs in alginate may further enhance their therapeutic effects by localizing and maintain the cells to the site of nerve injury and isolating them from a host immune response. Also, alginate hydrogel has been shown to affect encapsulated cell proliferation, secretion of therapeutic proteins, and increase mechanical stability of the NGC (Purcell et al. 2009).

Also, it was shown that laminin, present in the basement membrane of most cells, has the potential of promoting neurite outgrowth, survival, and attachment of neuronal cells (Wu et al. 2017).

After the injury, Schwann cells begin to proliferate along with nerve stump and this process alters the gene expression profile of Schwann cells (Zhang et al. 2017). In addition, Schwann cells have an essential role in the developmental and morphological property during the axonal repair. Mature Schwann cells were labeled with S100, but after peripheral nerve injury, they can back to an immature state and dedifferentiate to the myelinating Schwann cells, which elevate glial fibrillary acidic protein (GFAP) expression and the ability of regeneration of a nerve after injury (Zhang et al. 2017). In this study, a higher expression of S100 marker was found in the NGC filled with r-ADSCs, AuNPs, and BDNF, especially those containing alginate, which may be due to its protective effect.

Our real time RT-PCR results demonstrated that MBP marker has a high expression in Schwann-like cells in PLGBCA group compared with control and other conduit-implanted groups.

Besides, the expression of Schwann cells helps axon regeneration while the expression of NF200 may lead to nerve fiber regeneration.

Longitudinal sections showed that many NF200-positive regenerated axons have arrangement in the NGCs containing r-ADSCs with gold and BDNF nanoparticles, which especially incorporate with alginate hydrogel.

Our immunohistochemistry results agreed with behavioral analysis. As can be seen, the presence of BDNF, gold, and r-ADSCs encapsulated in alginate hydrogel improved better nerve recovery. In this regard, Galateanu et al. showed that the combination of hADSCs suspended with alginate hydrogel and cross-linked by calcium gluconate increased cell viability, proliferation, and differentiation in vitro. Moreover, they demonstrated that calcium gluconate successfully supported the adipogenesis and survival of hADSCs (Galateanu et al. 2012). Finally, the obtained results are encouraging and prove that therapy performed using PLGA nerve conduits with BDNF and AuNPs as an alternative to effective clinical procedures is viable, but more research is still needed. However, there are some factors that influence recovery following a nerve injury and regeneration such as time elapsed, proximity of the lesion to distal targets, patient age, and associated vascular or soft tissue damages.

Conclusion

Our findings show that the laminin-coated PLGA nerve conduit containing r-ADSCs, BDNF, and AuNPs significantly improves axonal regeneration and remyelination especially if suspended in alginate hydrogel and the combination of neurotrophic factor AuNPs, natural hydrogel, and stem cells may be synergistically enhancing axonal regeneration and remyelination. Our results suggest that simultaneous application of BDNF, AuNPs, and encapsulated ADSCs in the laminin-coated PLGA nerve conduit could be an effective treatment alternative for autologous nerve graft.

Acknowledgments The authors are grateful to Isfahan University of Medical Sciences.

Author Contributions MJ performed experimental work and preliminary writing of manuscript, SR designed the experiments and final revision, and RS, PR, and MK contributed to data collection and analyzed the data. All authors read and approved the final manuscript.

Funding This study was supported by Isfahan University of Medical Sciences, Isfahan, Iran.

Compliance with Ethical Standards

The study protocol was approved by ethical committee of Isfahan University of Medical Sciences.

Conflict of Interest The authors declare that they have no conflict of interest.

References

Augst AD, Kong HJ, Mooney DJ (2006) Alginate hydrogels as biomaterials. Macromol Biosci 6:623–633. https://doi.org/10.1002/mabi.200600069

Bain JR, Mackinnon SE, Hunter DA (1989) Functional evaluation of complete sciatic, peroneal, and posterior tibial nerve lesions in the rat. Plast Reconstr Surg 83:129–138. https://doi.org/10.1097/00006534-198901000-00024

Baltzis D, Meimeti E, Grammatikopoulou MG, Roustit M, Mavrogonatou E, Kletsas D et al (2018) Assessment of telomerase activity in leukocytes of type 2 diabetes mellitus patients having or not foot ulcer: possible correlation with other clinical parameters. Exp Ther Med 15:3420–3424. https://doi.org/10.3892/etm.2018.5798

Baranes K, Shevach M, Shefi O, Dvir T (2016) Gold nanoparticle-decorated scaffolds promote neuronal differentiation and maturation. Nano Lett 16:2916–2920. https://doi.org/10.1021/acs.nanolett.5b04033

Böcker A, Daeschler SC, Kneser U, Harhaus L (2019) Relevance and recent developments of chitosan in peripheral nerve surgery. Front Cell Neurosci 13:104. https://doi.org/10.3389/fncel.2019.00104

Boyd JG, Gordon T (2003) Glial cell line-derived neurotrophic factor and brain-derived neurotrophic factor sustain the axonal regeneration of chronically axotomized motoneurons in vivo. Exp Neurol 183:610–619. https://doi.org/10.1016/s0014-4886(03)00183-3

Brown JH, Das P, DiVito MD, Ivancic D, Tan LP, Wertheim JA (2018) Nanofibrous PLGA electrospun scaffolds modified with type I collagen influence hepatocyte function and support viability in vitro. Acta Biomater 73:217–227. https://doi.org/10.1016/j.actbio.2018.02.009

Campbell WW (2008) Evaluation and management of peripheral nerve injury. Clin Neurophysiol 119:1951–1965. https://doi.org/10.1016/j.clinph.2008.03.018

Chan JR, Cosgaya JM, Wu YJ, Shooter EM (2001) Neurotrophins are key mediators of the myelination program in the peripheral nervous system. Proc Natl Acad Sci U S A 98:14661–14668. https://doi.org/10.1073/pnas.251543398

Cornejo A, Sahar DE, Stephenson SM, Chang S, Nguyen S, Guda T, Wenke JC, Vasquez A, Michalek JE, Sharma R, Krishnegowda NK, Wang HT (2012) Effect of adipose tissue-derived osteogenic and endothelial cells on bone allograft osteogenesis and vascularization in critical-sized calvarial defects. Tissue Eng A 18:1552–1561. https://doi.org/10.1089/ten.TEA.2011.0515

Dinis T, Vidal G, Marin F, Kaplan D, Egles C (2013) Silk nerve: bioactive implant for peripheral nerve regeneration. Comput Methods Biomech Biomed Eng 16(Suppl 1):253–254. https://doi.org/10.1080/10255842.2013.815958

Dobrovolskaia MA, Patri AK, Zheng J, Clogston JD, Ayub N, Aggarwal P, Neun BW, Hall JB, McNeil SE (2009) Interaction of colloidal gold nanoparticles with human blood: effects on particle size and analysis of plasma protein binding profiles. Nanomedicine 5:106–117. https://doi.org/10.1016/j.nano.2008.08.001

Dziwenka M, Coppock R, Alexander M, Palumbo E, Ramirez C, Lermer S (2020) Safety assessment of a hemp extract using genotoxicity and oral repeat-dose toxicity studies in Sprague-Dawley rats. Toxicol Rep 7:376–385. https://doi.org/10.1016/j.toxrep.2020.02.014

Faroni A, Mobasseri SA, Kingham PJ, Reid AJ (2015) Peripheral nerve regeneration: experimental strategies and future perspectives. Adv Drug Deliv Rev 82-83:160–167. https://doi.org/10.1016/j.addr.2014.11.010

Galateanu B, Dimonie D, Vasile E, Nae S, Cimpean A, Costache M (2012) Layer-shaped alginate hydrogels enhance the biological performance of human adipose-derived stem cells. BMC Biotechnol 12:35. https://doi.org/10.1186/1472-6750-12-35

Gaudin R, Knipfer C, Henningsen A, Smeets R, Heiland M, Hadlock T (2016) Approaches to peripheral nerve repair: generations of biomaterial conduits yielding to replacing autologous nerve grafts in craniomaxillofacial surgery. Biomed Res Int 2016:3856262–3856218. https://doi.org/10.1155/2016/3856262

Georgiou M, Golding JP, Loughlin AJ, Kingham PJ, Phillips JB (2015) Engineered neural tissue with aligned, differentiated adipose-derived stem cells promotes peripheral nerve regeneration across a critical sized defect in rat sciatic nerve. Biomaterials 37:242–251. https://doi.org/10.1016/j.biomaterials.2014.10.009

Gurunathan S, Kim J-H (2018) Biocompatible gold nanoparticles ameliorate retinoic acid-induced cell death and induce differentiation in F9 teratocarcinoma stem cells. Nanomaterials 8:396. https://doi.org/10.3390/nano8060396

Hashimoto T, Suzuki Y, Kitada M, Kataoka K, Wu S, Suzuki K, Endo K, Nishimura Y, Ide C (2002) Peripheral nerve regeneration through alginate gel: analysis of early outgrowth and late increase in diameter of regenerating axons. Exp Brain Res 146:356–368. https://doi.org/10.1007/s00221-002-1173-y

Huang YC, Huang CC, Huang YY, Chen KS (2007) Surface modification and characterization of chitosan or PLGA membrane with laminin by chemical and oxygen plasma treatment for neural regeneration. J Biomed Mater Res A 82:842–851. https://doi.org/10.1002/jbm.a.31036

Ismail CAN, Suppian R, Ab Aziz CB, Long I (2020) Ifenprodil reduced expression of activated microglia, BDNF and DREAM proteins in the spinal cord following formalin injection during the early stage of painful diabetic neuropathy in rats. J Mol Neurosci 1–15. https://doi.org/10.1007/s12031-020-01661-1

Jahromi M, Razavi S, Bakhtiari A (2019) The advance on nerve tissue engineering: from fabrication of nerve conduit to in vivo nerve regeneration assays. J Tissue Eng Regen Med 13:2077–2100. https://doi.org/10.1002/term.2945

Jiang G, Xiao G, Luo C, Tang Z, Teng Z, Peng X (2020) Correlation between SNPs at the 3′UTR of the FGF2 gene and their interaction with environmental factors in Han Chinese diabetic peripheral neuropathy patients. J Mol Neurosci 1–12. https://doi.org/10.1007/s12031-020-01641-5

Jing W, Ao Q, Wang L, Huang Z, Cai Q, Chen G, Yang X, Zhong W (2018) Constructing conductive conduit with conductive fibrous infilling for peripheral nerve regeneration. Chem Eng J 345:566–577. https://doi.org/10.1016/j.cej.2018.04.044

Kara M, Oztas E, Ramazanoğulları R, Kouretas D, Nepka C, Tsatsakis AM, Veskoukis AS (2020) Benomyl, a benzimidazole fungicide, induces oxidative stress and apoptosis in neural cells. Toxicol Rep 7:501–509. https://doi.org/10.1016/j.toxrep.2020.04.001

Katsarou MS, Karakonstantis K, Demertzis N, Vourakis E, Skarpathioti A, Nosyrev AE, Nosyrev AE, Tsatsakis A, Kalogridis T, Drakoulis N (2017) Effect of single-nucleotide polymorphisms in ADH 1B, ADH 4, ADH 1C, OPRM 1, DRD 2, BDNF, and ALDH 2 genes on alcohol dependence in a Caucasian population. Pharmacol Res Perspect 5:e00326. https://doi.org/10.1002/prp2.326

Keshavarz M, Moloudi K, Paydar R, Abed Z, Beik J, Ghaznavi H, Shakeri-Zadeh A (2018) Alginate hydrogel co-loaded with cisplatin and gold nanoparticles for computed tomography image-guided chemotherapy. J Biomater Appl 33:161–169. https://doi.org/10.1177/0885328218782355

Li R, Li Y, Wu Y, Zhao Y, Chen H, Yuan Y, Xu K, Zhang H, Lu Y, Wang J, Li X, Jia X, Xiao J (2018) Heparin-poloxamer thermosensitive hydrogel loaded with bFGF and NGF enhances peripheral nerve regeneration in diabetic rats. Biomaterials 168:24–37. https://doi.org/10.1016/j.biomaterials.2018.03.044

Li R, Li D-h, Zhang H-y, Wang J, Li X-k, Xiao J (2020) Growth factors-based therapeutic strategies and their underlying signaling mechanisms for peripheral nerve regeneration. Acta Pharmacol Sin 1–12. https://doi.org/10.1038/s41401-019-0338-1

Lin Y-L, Jen J-C, Hsu S-h, Chiu M (2008) Sciatic nerve repair by microgrooved nerve conduits made of chitosan-gold nanocomposites. Surg Neurol 70:9–18. https://doi.org/10.1016/j.surneu.2008.01.057

Ma PX, Elisseeff J (2005) Scaffolding in tissue engineering. CRC Press

McGregor CE, English AW (2019) The role of BDNF in peripheral nerve regeneration: activity-dependent treatments and Val66Met. Front Cell Neurosci 12:522. https://doi.org/10.3389/fncel.2018.00522

Ostrowski AD, Martin T, Conti J, Hurt I, Harthorn BH (2009) Nanotoxicology: characterizing the scientific literature, 2000–2007. J Nanopart Res 11:251–257. https://doi.org/10.1007/s11051-008-9579-5

Pabari A, Lloyd-Hughes H, Seifalian AM, Mosahebi A (2014) Nerve conduits for peripheral nerve surgery. Plast Reconstr Surg 133: 1420–1430. https://doi.org/10.1097/PRS.0000000000000226

Patel NP, Lyon KA, Huang JH (2018) An update–tissue engineered nerve grafts for the repair of peripheral nerve injuries. Neural Regen Res 13:764–774. https://doi.org/10.4103/1673-5374.232458

Paviolo C, Stoddart PR (2017) Gold nanoparticles for modulating neuronal behavior. Nanomaterials (Basel) 7:92. https://doi.org/10.3390/nano7040092

Purcell EK, Singh A, Kipke DR (2009) Alginate composition effects on a neural stem cell–seeded scaffold. Tissue Eng Part C: Methods 15: 541–550. https://doi.org/10.1089/ten.tec.2008.0302

Razavi S, Seyedebrahimi R, Jahromi M (2019) Biodelivery of nerve growth factor and gold nanoparticles encapsulated in chitosan nanoparticles for Schwann-like cells differentiation of human adipose-derived stem cells. Biochem Biophys Res Commun 513:681–687. https://doi.org/10.1016/j.bbrc.2019.03.189

Reid AJ, Sun M, Wiberg M, Downes S, Terenghi G, Kingham PJ (2011) Nerve repair with adipose-derived stem cells protects dorsal root ganglia neurons from apoptosis. Neuroscience 199:515–522. https://doi.org/10.1016/j.neuroscience.2011.09.064

Schuh CM, Morton TJ, Banerjee A, Grasl C, Schima H, Schmidhammer R et al (2014) Activated Schwann cell-like cells on aligned fibrin-poly(lactic-co-glycolic acid) structures: a novel construct for application in peripheral nerve regeneration. Cells Tissues Organs 200: 287–299. https://doi.org/10.1159/000437091

Seyedebrahimi R, Razavi S, Varshosaz J (2019) Controlled delivery of brain derived neurotrophic factor and gold-nanoparticles from chitosan/TPP nanoparticles for tissue engineering applications. J Clust Sci 31:99–108. https://doi.org/10.1007/s10876-019-01621-9

Seyedebrahimi R, Razavi S, Varshosaz J, Vatankhah E, Kazemi M (2020) Beneficial effects of biodelivery of brain-derived neurotrophic factor and gold nanoparticles from functionalized electrospun PLGA scaffold for nerve tissue engineering. J Clust Sci. https://doi.org/10.1007/s10876-020-01822-7

Shanbhag MS, Lathia JD, Mughal MR, Francis NL, Pashos N, Mattson MP, Wheatley MA (2010) Neural progenitor cells grown on hydrogel surfaces respond to the product of the transgene of encapsulated genetically engineered fibroblasts. Biomacromolecules 11:2936–2943. https://doi.org/10.1021/bm100699q

Shukla R, Bansal V, Chaudhary M, Basu A, Bhonde RR, Sastry M (2005) Biocompatibility of gold nanoparticles and their endocytotic fate inside the cellular compartment: a microscopic overview. Langmuir 21:10644–10654. https://doi.org/10.1021/la0513712

Singh P, Pandit S, Mokkapati V, Garg A, Ravikumar V, Mijakovic I (2018) Gold nanoparticles in diagnostics and therapeutics for human cancer. Int J Mol Sci 19:1979. https://doi.org/10.3390/ijms19071979

Siokas V, Kardaras D, Aloizou A-M, Asproudis I, Boboridis KG, Papageorgiou E, Hadjigeorgiou GM, Tsironi EE, Dardiotis E (2019) BDNF rs6265 (Val66Met) polymorphism as a risk factor for blepharospasm. NeuroMolecular Med 21:68–74. https://doi.org/10.1007/s12017-018-8519-5

Sivolella S, Brunello G, Ferrarese N, Della Puppa A, D'Avella D, Bressan E, Zavan B (2014) Nanostructured guidance for peripheral nerve injuries: a review with a perspective in the oral and maxillofacial area. Int J Mol Sci 15:3088–3117. https://doi.org/10.3390/ijms15023088

Vaezifar S, Razavi S, Golozar MA, Esfahani HZ, Morshed M, Karbasi S (2015) Characterization of PLGA/chitosan electrospun nanobiocomposite fabricated by two different methods. Int J Polym Mater Polym Biomater 64:64–75. https://doi.org/10.1080/00914037.2014.886244

Wang T, Ito A, Aoyama T, Nakahara R, Nakahata A, Ji X, Zhang J, Kawai H, Kuroki H (2018) Functional evaluation outcomes correlate with histomorphometric changes in the rat sciatic nerve crush injury model: a comparison between sciatic functional index and kinematic analysis. PLoS One 13:e0208985. https://doi.org/10.1371/journal.pone.0208985

Wei X, Du Z, Zhao L, Feng D, Wei G, He Y et al (2009) IFATS collection: the conditioned media of adipose stromal cells protect against hypoxia-ischemia-induced brain damage in neonatal rats. Stem Cells 27:478–488. https://doi.org/10.1634/stemcells.2008-0333

Wu T, Li D, Wang Y, Sun B, Li D, Morsi Y (2017) Laminin-coated nerve guidance conduits based on poly(l-lactide-co-glycolide) fibers and yarns for promoting Schwann cells' proliferation and migration. J Mater Chem B 5:3186–3194. https://doi.org/10.1039/C6TB03330J

Zarinfard G, Tadjalli M, Razavi S, Kazemi M (2016) Effect of laminin on neurotrophic factors expression in Schwann-like cells induced from human adipose-derived stem cells in vitro. J Mol Neurosci 60:465–473. https://doi.org/10.1007/s12031-016-0808-6

Zhang R, Rosen JM (2018) The role of undifferentiated adipose-derived stem cells in peripheral nerve repair. Neural Regen Res 13:757–763. https://doi.org/10.4103/1673-5374.232457

Zhang S-j, Wu W-l, Yang K-y, Chen Y-z, Liu H-c (2017) Phenotypic changes of Schwann cells on the proximal stump of injured peripheral nerve during repair using small gap conduit tube. Neural Regen Res 12:1538–1543. https://doi.org/10.4103/1673-5374.215266

Zhuang H, Bu S, Hua L, Darabi MA, Cao X, Xing M (2016) Gelatin-methacrylamide gel loaded with microspheres to deliver GDNF in bilayer collagen conduit promoting sciatic nerve growth. Int J Nanomedicine 11:1383–1394. https://doi.org/10.2147/IJN.S96324